

H and D depth profiles in implanted and laser-annealed beryllium

F. Schiettekatte *, D. Kéroack, G.G. Ross and B. Terreault

INRS-Énergie et Matériaux, Université du Québec, C.P. 1020, Varennes, Québec, Canada J3X 1S2

The thermodynamic properties of H and D implanted in Be to different fluences have been investigated by laser flash desorption. From the evolution of the H and D depth profiles following laser annealing, different detrapping/diffusion processes in matter are proposed. The experimental results were compared to those obtained from a finite element time resolved simulation code. Two different processes depending on the H or D fluence can be inferred: at low fluence, a 1.7 eV/molecule detrapping energy and a fairly high effective diffusion coefficient have to be involved, while at high fluence the detrapping energy is ≤ 1 eV/molecule and an extremely rapid migration have to be considered. The transition between these two regimes corresponds approximately to the fluence for which blistering becomes detectable.

1. Introduction

There are limited data on hydrogen isotope behaviour in beryllium, in spite of its recent use as a plasma facing material in fusion devices [1]. Thermal desorption experiments can give much information about the thermodynamic properties of foreign atoms in matter. For instance, Wampler [2] found with this method evidence for two traps for implanted D in Be, i.e. a strong trap of 1.8 eV at atom ratios D/Be ≤ 5 –10%, and a weaker trap of 1.0 eV at higher ratios; desorption was not limited by diffusion. There are conflicting data on the diffusivity, but the recent results of Abramov et al. [3], which take into account the surface oxide in the data analysis, give $D = 6.7 \times 10^{-5} \exp(-0.29 \text{ eV}/kT) \text{ cm}^2/\text{s}$ for the D diffusion coefficient in Be.

In recent years, laser flash desorption has been applied [4] to near-surface implanted ions, providing some important advantages (negligible desorption from sample bulk and none from sample holder, desorption time negligible compared to pumping or wall degassing time). But the most important features come from the short heating time (e.g. 10 ns) followed by the rapid quench (≤ 100 ns) [5]. Consequently, the thermodynamic properties can be investigated in different conditions than in slow annealing, favoring the kinetics of the process against the energetics (which dominate under equilibrium conditions). A quantitative kinetic simulation [5] of the desorption process can be used to deduce its fundamental parameters. In previous inves-

tigations, the quantities of desorbed gas were measured for H [6] and D [7] implanted in Be. In ref. [7], a trapping energy of 1.7 eV was found for atom ratios up to 11%, consistent with Wampler's strong trap. In addition, the laser desorption process was found to be simultaneously limited by detrapping *and* diffusion; a value of $D = (8 \pm 1) \times 10^{-4} \exp(-0.32 \pm 0.02 \text{ eV}/kT) \text{ cm}^2/\text{s}$ was fitted to the data. This is an order of magnitude higher than Abramov's value, which was already higher than the earlier results. Moreover, at concentrations above 11%, the data could not be fitted by using Wampler's two trapping energies.

Depth profiling of partially desorbed samples can provide essential additional information [5]. For instance, in this way, limitation by diffusion would be directly manifested by profile broadening, and not only inferred from a mathematical fit to gas evolution data. Similarly, a surface barrier would give rise to a flat and very wide profile, and retrapping by defects to a shift of the peak of the profile. The above mentioned difficulty in fitting the high fluence data [7] makes it even more important to obtain new information by another technique. This paper describes a study of the profile modification after pulsed-laser desorption of H and D implanted in Be at medium to high fluences.

2. Procedures

Samples of hot rolled Be of $> 99.8\%$ purity have been polished by means of a SiO₂ suspension with a finish of 0.04 μm . Rutherford backscattering analysis showed the presence of $\approx 1 \times 10^{16}$ O atoms/cm² at the surface (equivalent BeO thickness = 1.4 nm). After

* Corresponding author, tel. +1 514 449 8130, fax +1 514 449 8102, e-mail schiette@iris1.inrs-ener.quebec.ca.

ultrasonic cleaning in CCl_4 , acetone and methanol, the samples were introduced into the implantation chamber where the base pressure was 5×10^{-8} Torr. They were implanted with magnetically selected H_3^+ or D_3^+ ions of energy ranging from 0.7 to 1.5 keV/amu and fluences from 0.2×10^{17} at/cm² to 1.9×10^{17} at/cm². The mean ranges are 21 to 38 nm (\gg oxide thickness).

The samples were transferred in air to the laser desorption chamber where the base pressure is maintained below 1×10^{-8} Torr by means of an ion pump and a cryogenic trap. They were irradiated by a Q-switched ruby laser, having a Gaussian pulse of 25 ns FWHM. The D and/or H partial pressure was accurately measured by a quadrupole mass spectrometer. The experimental setup is described in ref. [8]. The laser energy was varied from 0.1 to 2.1 J/cm². Most of the laser shots were directed to different locations on the substrate, but for some experiments, successive shots of increasing energy were accumulated on the same spot (hereafter named “ramp”).

Depth profiling was performed on irradiated and non-irradiated zones by means of the ERD $E \times B$ technique [9]. The 350 keV probing beam was ^4He for H profiling and ^3He for D profiling. Since the ion beam can also induce desorption, the fluence was limited to $\approx 2.5 \times 10^{15}$ He/cm². The profiles were corrected for the depth varying resolution by means of a deconvolution procedure which uses constrained B-spline and delta-function [10].

The desorption data and the depth profiles were compared to the kinetic simulations performed with the code DTRLAS [5], whose free parameters were varied until agreement with both sets of data was found. Very briefly, the photon absorption and the heat flow are calculated accurately as a function of time and space by finite differences. In addition, at each time step, the H or D evolution is simulated according to the following equations:

$$\text{– detraping: } \partial C_T / \partial t = -\nu V^{n-1} C_T^n,$$

$$\text{with } \nu = \nu_0 \exp(-E_B/kT);$$

$$\text{– diffusion: } D = D_0 \exp(-E_D/kT),$$

where C_T is the trapped concentration and T the space and time dependent temperature. The parameters are the frequency factors νV^{n-1} and D_0 , the reaction order n , and the activation energies E_B and E_D . In addition, bulk and surface retrapping and surface recombination and desorption are simulated, but are not detailed here since they were not found to be rate-limiting. The measured H or D implantation profiles are used as initial profiles; each successive laser shot is simulated using its measured laser energy and the calculated quenched profile obtained at the end of the preceding shot after the material has cooled down.

3. Results and discussion

The saturation concentration, measured by the ERD $E \times B$ method, is reached for a fluence of 0.4×10^{17} at./cm² for both H and D implanted with an energy near 1 keV into Be. The samples implanted with fluences beyond this limit contained less H or D than just saturated samples, which suggests gas release from blister exfoliation in oversaturated samples. Fig. 1 shows two examples of D desorption by laser for low (Fig. 1a) and high (Fig. 1b) fluences of D implanted in Be. Laser shots of increasing energy were fired at the same position on the sample. When D is implanted at low fluence, desorption starts at a threshold of 0.6 J/cm², and the process is well fitted by a simulation using the detrapping and diffusion coefficients reported in ref. [7] and quoted above. However, when D is implanted at high fluence, the desorption process begins well below the previous threshold. It can be reproduced by two different models. One is a detrapping-limited model in which two traps of 1.0 and 0.8 eV (maybe actually a distribution of traps) are initially populated, and in which the detrapped molecules instantaneously migrate to the surface and desorb (suggestive of a short-cut to the surface). The second is a diffusion-limited model with a low activation energy (0.18 eV). However, in this case, simulations show that the diffusion process would transport a large part of the D atoms deeper into the bulk and so, the mean depth of the profile would be strongly shifted. Fig. 2 shows the measured and the simulated D depth profiles corresponding to this experiment. It is clear that the experimental depth profiles are much better reproduced by the two-trap desorption model than by the diffusion-limited model.

Fig. 3 shows results of the profile evolution following laser desorption of H implanted to different flu-

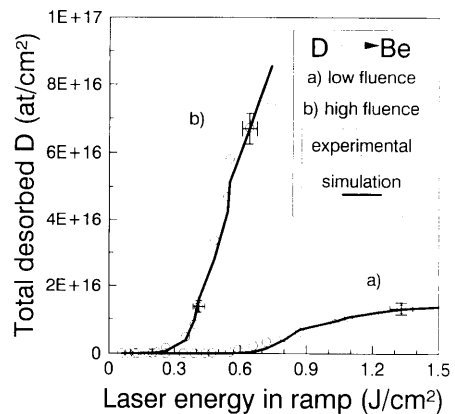


Fig. 1. Cumulative release of D implanted in Be after desorption by laser energy ramp: (a) 0.4 keV, 1.75×10^{16} D/cm². (b) 1 keV, 1.1×10^{17} D/cm².

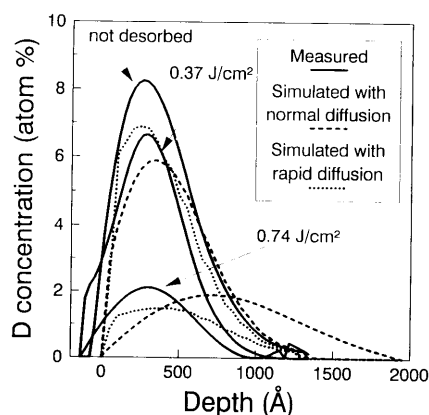


Fig. 2. Depth profile evolution after laser energy shot of 0.37 J/cm^2 and energy ramp to 0.74 J/cm^2 : experimental (—), and simulated with diffusion-limited (-----) and detrapping-limited (·····) processes. The Be sample was implanted at 1 keV with $1.1 \times 10^{17} \text{ D/cm}^2$.

ences into Be. In Fig. 3a, the H was implanted with a fluence of $0.42 \times 10^{17} \text{ H/cm}^2$ at 1.5 keV. A single laser shot with an energy of 1.7 J/cm^2 was used. The evolution of the measured H profile is reproducible when the same parameters as for D at low fluence are used. In Figs. 3b and 3c, H was implanted with an energy of 1.5 keV and a fluence of $1.5 \times 10^{17} \text{ H/cm}^2$, and with an energy of 0.7 keV and a fluence of $0.9 \times 10^{17} \text{ H/cm}^2$, respectively. One single laser shot of 0.5 J/cm^2 and an energy ramp to 0.9 J/cm^2 (0.8 J/cm^2 for Fig. 3c) were used. Both profile evolutions were reproduced by means of two traps with energies of 0.9 and 0.6 eV/molecule. As it was observed for D behaviour in Be (Fig. 1), the gas desorption curves can be reproduced by a detrapping-limited model with an instantaneous migration to the surface, or with a diffusion-limited model that is weakly activated (0.1 eV). Mean depths and variances of the measured depth profiles as well as those obtained from the simulated profiles according to the diffusion-limited and the detrapping-limited models are compared in Table 1. It is

Table 1

Mean depths and variances for the profiles in Figs. 3b and 3c: measured values calculated from the experimental profiles; “detrapping” and “diffusion” values obtained from the profiles simulated with detrapping-limited and diffusion-limited models respectively

Laser energy	Mean depth [\AA]			Variance [\AA]		
	Measured	Detrapping	Diffusion	Measured	Detrapping	Diffusion
Fig. 3b, 0.5 J/cm^2 shot	505	424	678	216	244	478
Fig. 3b, 0.9 J/cm^2 ramp	526	562	996	280	280	443
Fig. 3c, 0.5 J/cm^2 shot	378	345	632	171	192	363
Fig. 3c, 0.5 J/cm^2 ramp	349	350	840	189	195	431
Fig. 3c, 0.8 J/cm^2 ramp	445	435	994	190	232	443

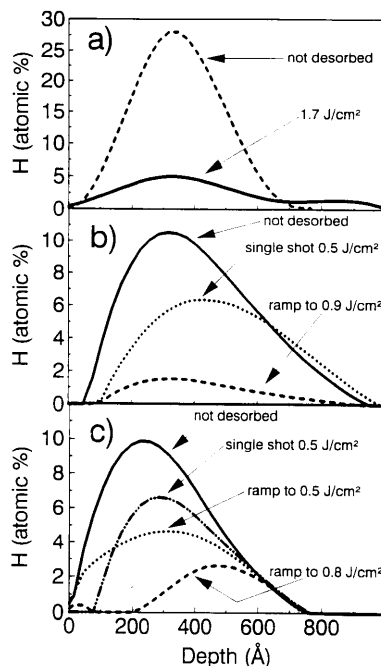


Fig. 3. Depth profiles of H implanted in Be at an energy of 1.5 keV: (a) $4.2 \times 10^{16} \text{ H/cm}^2$ and desorbed with a single laser shot of 1.7 J/cm^2 , (b) $1.5 \times 10^{17} \text{ H/cm}^2$ and desorbed with a single laser shot of 0.5 J/cm^2 and by an energy ramp to 0.9 J/cm^2 ; (c) $9 \times 10^{16} \text{ H/cm}^2$ (energy of 0.7 keV) and desorbed with a single laser shot of 0.5 J/cm^2 and by energy ramps to 0.5 J/cm^2 and to 0.8 J/cm^2 .

clear that the detrapping-limited model is the most appropriate.

This last fact is confirmed by Fig. 4 which shows the normalised gas desorption curves corresponding to the profiles (ramp) in Figs. 3b and c. Although the two implantations were done at two different energies (1.5 and 0.7 keV, mean ranges of 38 nm and 21 nm) the desorption curves coincide, which means that the desorption is not diffusion-limited.

The detrapping energy found for H or D implanted at low fluence (1.7 eV) is consistent with that of

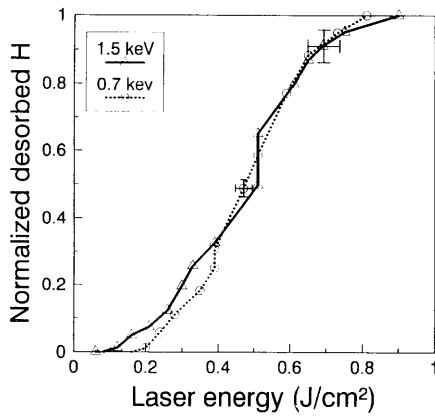


Fig. 4. Normalized hydrogen release after laser desorption from a Be sample implanted with two different energies of 0.7 keV (○) and 1.5 keV (△).

Wampler's [2] strong trap (1.8 eV), while the activation energies found at high fluence (0.6 to 1.0 eV) are fairly close to that of his weak trap (1.0 eV). According to Wampler the strong trap was filled first (up to a D/Be atom ratio of 5–10%), followed by filling of the weak trap until its saturation. However, none of our data can be similarly described by two well separated stages. Rather, it appears that when the strong trap becomes oversaturated (for D/Be \geq 14%), a transition takes place which leaves *all* the H or D more loosely bound. It remains to be seen if this difference is connected with the rapid heating and quench produced by the laser. Ongoing microscopy work is aimed at studying this question [11]. The two different types of detrapping occur at fluence values comparable to, but somewhat less than, those for which blistering starts to be clearly observed. Then the desorption process which was diffusion-limited becomes independent of the diffusion. In addition, the laser desorption of such samples caused dislocation lines ending on grain boundaries to appear [11]. These lines could facilitate the H and D migration from the bulk of the material to the grain boundaries and then to the surface. More work, especially microscopy, is needed to characterize the desorption mechanism in the high fluence domain.

4. Summary

We have performed laser desorption of H and D implanted in Be at various fluences around 1×10^{17} at/cm² with energies near 1 keV, and measured the H

or D depth profiles at various stages of the process. When H or D are implanted at low fluences ($< 0.5 \times 10^{17}$ at/cm²), the evolution of the profile is correctly described by a single trap and a diffusion-like process as described in ref. [7]. On the other hand, for high fluences, where blistering and cracking appear, the trapping energies are shifted from 1.7 eV to below 1 eV/molecule. Moreover, a comparison between measured and simulated H or D depth profiles before and after the laser desorption shows that the process becomes independent of the diffusion (direct migration to the surface) and is limited by detrapping only. This observation is confirmed by the behaviour of the desorption yield versus laser energy which is the same for two different energies of implantation.

Acknowledgements

We thank J. Pelletier for the excellent operation of the accelerator and P. Zheng for fruitful discussions. This research benefited from grants from the National Science and Engineering Research Council.

References

- [1] K.J. Dietz and the JET Team, *Fusion Technol.* 19 (1991) 2031.
- [2] W.R. Wampler, *J. Nucl. Mater.* 122 (1984) 1598.
- [3] E. Abramov, M.P. Riehm and D.A. Thompson, *Nucl. Instr. and Meth.* 175 (1990) 90.
- [4] G.G. Ross, B. Terreault, C. Boucher and R. Boivin, *J. Vac. Sci. Technol. A* 4 (1986) 1243.
- [5] B. Terreault, *J. Appl. Phys.* 62 (1987) 152.
- [6] R. Boivin and B. Terreault, *J. Nucl. Mater.* 187 (1992) 117.
- [7] D. Kéroack and B. Terreault, Laser desorption study of deuterium implanted in beryllium, accepted for Proc. 6th Int. Conf. on Fusion Reactor Materials, Stresa, Italy, 1993.
- [8] R. Boivin, G.G. Ross and B. Terreault, *J. Appl. Phys.* 73 (1993) 1936.
- [9] G.G. Ross and L.L. Leblanc, *Nucl. Instr. and Meth. B* 26 (1992) 484.
- [10] F. Schiettekatte, R. Marchand and G.G. Ross, Deconvolution of noisy data with strong discontinuity and uncertainty evaluation, submitted to *Nucl. Instr. and Meth.*
- [11] P. Zheng, private communication; K. Touhouche, presented at the Materials Research Society Symposium, Boston, USA, 1993.